WELDING RESEARCH

SUPPLEMENT TO THE *WELDING JOURNAL,* MAY 2007
Sponsored by the American Welding Society and the Welding Research Council

Optimum Evaluation for Electron Beam Weldments of AZ61A-F Extruded Plates

Seventy-seven sets of specimens were joined by changing variables to determine the optimum parameters for welding 11-mm AZ61A alloy

BY CHAO-TING CHI AND CHUEN-GUANG CHAO

ABSTRACT. Recently there has been a renewed interest in magnesium alloys because of their extensive applications in industries, such as computing, communications, consumer electronics, aerospace, and traffic. However, the plastic deformation of these alloys is restricted because HCP magnesium has fewer dislocation slip systems. This limitation can be circumvented by dividing shape-complicated workpieces into several more easily made parts, which are then combined into one. Due to the interaction between material properties and welding conditions, there are various kinds of defects in the welds of magnesium alloys, and these defects cause obvious stress concentrations and serious material damage. This study used a custom-made 11-mm-thick AZ61A extruded plate. By operating and comparing the variable parameters of electron beam welding (EBW), the condition was optimized for ultimate tensile strength (UTS) at 100 mA, 50 kV, 60.6 mm/s, and a focal position at the bottom of the workpiece. Under these conditions, ultimate tensile strengths of 83% and 96%, respectively, were obtained for the base metal in weldments with and without stress concentrators on their surface. For worse conditions such as 100 mA, 45 kV, 86.0 mm/s, and a focal position at the bottom, the UTS of electron beam weldments for AZ61A-F plates was reduced by the three factors of root concavity, heat-affected zone (HAZ), and cavities.

*CHAO-TING CHI (*joseph.mse92g@nctu.edu.tw*) is with Department of Materials Science and Engineering, National Chiao-Tung University, Taiwan, ROC., and the System Manufacturing Center, Chun Shan Institute of Science and Technology, Taipei, Taiwan, ROC. CHUEN-GUANG CHAO (*c_g_chao@hotmail.com*) is with Department of Materials, Science and Engineering, National Chiao-Ting University, Taiwan, ROC.*

Introduction

Of the lightweight metals, magnesium alloys are important structural materials due to their properties of low density and high specific strength. Magnesium alloys are readily available since pure magnesium can be extracted from sea water or reduced from magnesite and dolomite. In addition, the surface treatment of magnesium alloys has been extensively researched and developed using both physical and chemical methods. Therefore, the use of different magnesium alloys has steadily increased, and at this point AZ series magnesium alloys (Al content is below 11.5 wt-%) are the most commonly used. In this series, AZ61 plays a very significant role due to its optimal combination of strength and ductility, which results from being heat treatable as Al content is above 6 wt-% (Ref. 1).

The plastic deformation of AZ61 alloys is restricted because hexagonal close-packed (HCP) magnesium has fewer dislocation slip systems. It cannot be extensively formed, and if fabricated into shape-complicated parts or assemblies, it will fail relatively easily. Although this problem can be solved by using die casting, the average price of each facture will be increased significantly for fractional production because of lower product reliability and more expensive dies. Moreover, die casting is a mass product process with poor mechanical properties in comparison with the extrusion process. In order to reduce the extent of plastic deformation and to raise the mechanical properties, a shape-complicated workpiece can be divided into several simple structural forging parts that are then combined into one. This method will effectively improve problems with forming.

KEYWORDS

Electron Beam Welding
Heat-Affected Zone
Lightweight Metals
Magnesium Alloys
Stress Concentration
Weld Tensile Strength

Particularly in the aerospace and national defense industries, it is important to select a suitable way to join various parts and assemblies. Welding and mechanical fastening are mostly used in these situations. Compared to mechanical fastening, welding usually provides better performance. However, interface junctions are still the major issues since many weld failures result from them. Because high-energy-density beam welding (HBW) has much higher precision, greater depth-to-width ratio of the weld, lower net heat input, narrower HAZ, and finer microstructure as compared with conventional welding (such as GTAW) (Ref. 2), it can be adopted in order to reduce the failure probability of parts and assemblies.

Generally speaking, HBW is very suitable for the welding of magnesium alloys, although it requires the use of a flux or a vacuum environment to protect the molten metal due to the high reactivity of magnesium alloys. Overall, most studies of HBW of magnesium alloys have concentrated on laser welding (Refs. 3–5). Though laser welding is a very convenient process, its maximum depth of complete join penetration (limited by the tolerance of optical device for beam power) is smaller than that of electron beam welding (EBW), and this consideration generally makes EBW the most effective technique for attaching pieces.

Electron beam welding, which achieves the highest precision in position and forms

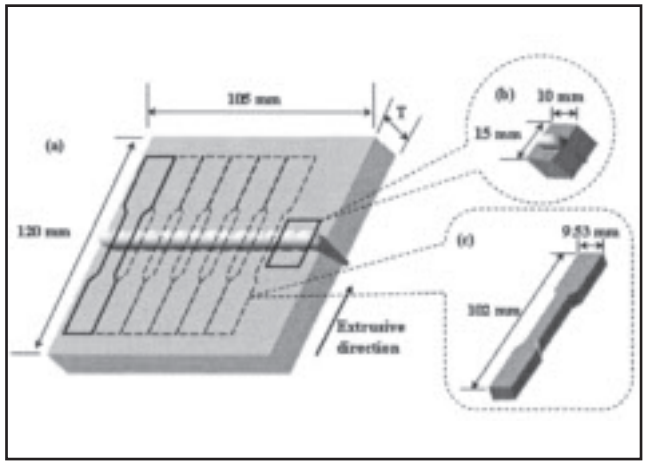

Fig. 1 — Sketch of EB-welded magnesium alloy specimen for different testing purposes.

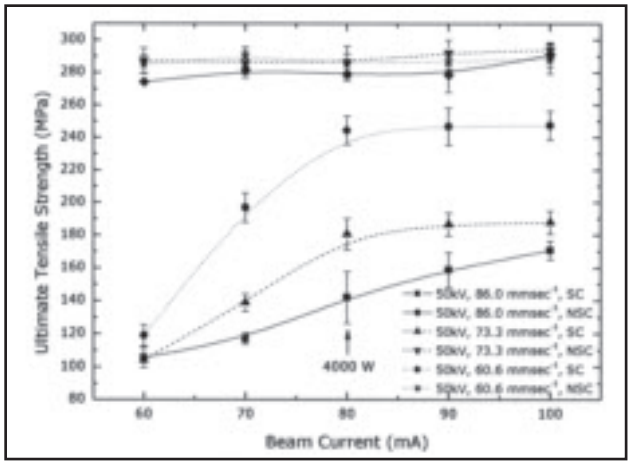

Fig. 2 — Effects of beam current and welding speed on the UTS of AZ61A weldments. Curves are linked by parameters A, E, J, O, and U with individual welding speed. Base metal UTS is 297.4 MPa.

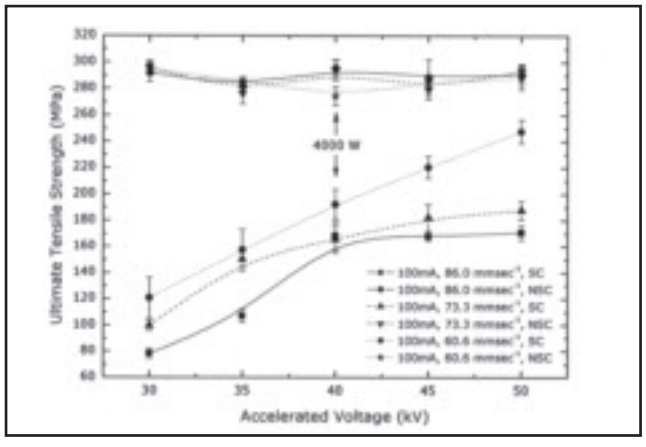

Fig. 3 — Effects of accelerated voltage and welding speed on the UTS of AZ61A weldments. Curves are linked by parameters A, F, K, Q, and W with individual welding speed. Base metal UTS is 297.4 MPa.

the highest depth-to-width ratio of a weld, was developed in 1950s and used in the nuclear industry (Ref. 6). In the early stages of EBW development, since its equipment required high vacuum levels, it was not used extensively because of the high cost and low productivity. From research over the last several decades, low vacuum and nonvacuum systems were developed to greatly reduce the working time (Ref. 7). So far, EBW has been applied to the automobile, aerospace, and national defense industries. Maybe it is possible that EBW of magnesium alloys will become the primary technology of lightweight alloys.

The melted magnesium alloys have higher vapor pressure and better fluidity than the melted aluminum or iron alloys. This reduces the stability of the weld pool surface and its process window (Ref. 9). Furthermore, imperfect parameter condition with asymmetrical Gaussian distribution of input energy (Ref. 10) and additions of unsuitable elements such as excessive Zn (above 1 wt-%) (Ref. 1) caused defects in the fusion zone (FZ) of weldments, which could seriously influence the weld mechanical properties. Presently, there have been only a few studies on EBW of magnesium alloys (Refs. 8, 10–12), which is generally due to the high cost of EBW equipment and magnesium alloys for academic research. Therefore, it is worth examining this subject more closely.

The authors adjusted the variable parameters of EBW including beam current, acceleration voltage, welding speed, and focal position. Accordingly, 77 sets of custom-made specimens of 11-mm-thick AZ61A extruded plate were fabricated and examined in a comparative study.

Experimental Procedure

In this study, the research material used was custom-made AZ61A extruded plate, which had a dimension of 105 × 60 × 12 mm (Ref. 3). The surface, bottom, and side of the AZ61A-F plate were removed to a thickness of 0.5 mm to avoid influence of the oxide layer. After being stored in a vacuum desiccator (10^{-3} torr) for three days, the AZ61A-F plates were welded together with a low-voltage EBW machine for a final dimension of 105 × 120 × 11 mm (Ref. 3) — Fig. 1A. The variable parameters of EBW were arranged and combined in turn according to five fixed power values (3000, 3500, 4000, 4500, and 5000 W) under high vacuum (3 × 10^{-5} torr). The two parameters have three major repeated values (beam current of 100, 125, 150 mA and accelerating voltage of 30, 40, 50 kV) and some minor nonrepeated values in their specific regions (beam current of 60–167 mA and accelerating voltage of 20–50 kV). The conditions of welding speed (60.6, 73.3, and 86.0 mm/s) and the focal position (bottom [0 mm] of the plate) remained the same. Only one parameter was changed at a time in order to study the individual characteristic of these parameters. A weldment with maximum UTS can be selected from them, and then compared with focusing at the surface (+11.0 mm) and middle (+5.5 mm) of the plate. All parameter combinations are indicated in Table 1. Accordingly, 77 sets of specimens (i.e., 3 × 25 + 2 = 77) were fabricated and examined for comparison.

The direction of all welds was perpendicular to that of the extrusion. These weldments were cut into one metallographic sample (Fig. 1B) and six tensile specimens (Fig. 1C). Three of the specimens had a milled finish on the top and bottom surfaces as nonstress concentration (NSC) specimens, while the other three retained the original weld feature as stress concentration (SC) specimens. These specimens, whose detailed dimensions were according to ASTM B557-02 standard specification (Ref. 13), were used for comparing the influence of stress concentration. In particular, the weld should be perpendicular to the longitudinal direction of the standard tensile specimens and located at the center of gauge length to achieve precise measurement of the weld strength. Additionally, after microstructure inspection, the metallographic specimen was divided into two pieces along the central line of the weld

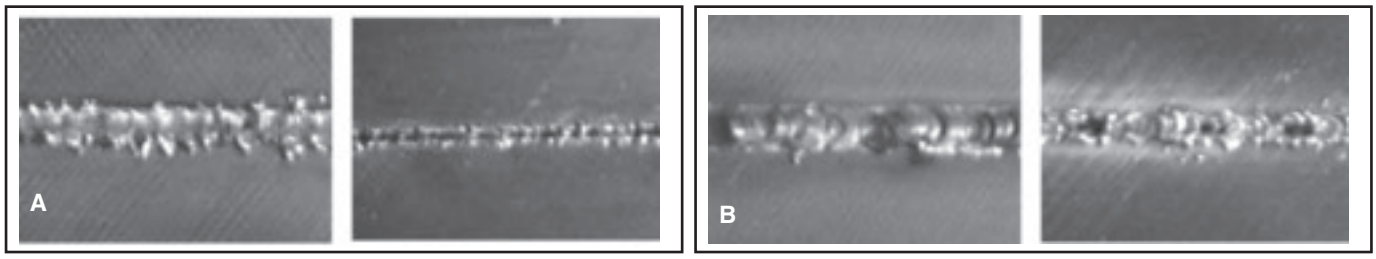

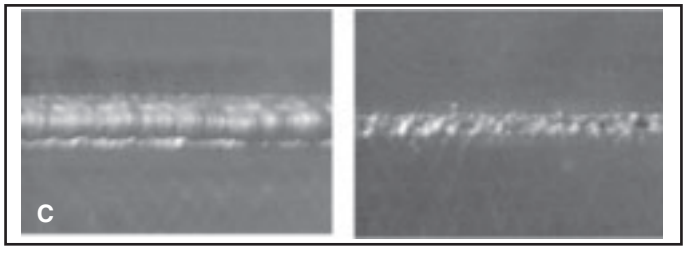

Fig. 4 — Comparison of weld appearance at different focal positions of AZ61A-F plates. Fixed conditions are 100 mA, 50 kV, and 60.6 mm/s. A — Focus at surface; B — Focus at middle; C — Focus at bottom. (crest and root respectively)

cross section. Thus the phase of the transverse plane of the extruded plate could be identified by x-ray diffraction (XRD).

Except for the foregoing inspections, the assessment of postwelding characterization of the workpiece also included chemical composition analysis of the material and distribution of micro-indentation hardness (Vickers, HV) on the transverse plane. The optimum parameters for maximum value of UTS were obtained in accordance with these experimental results.

Results and Discussions

Chemical Composition Analysis

The chemical compositions of AZ61A-F plate were analyzed using inductively coupled plasma-atom emission spectrometer and mass spectrometer (ICP-AES and ICP-MS). As shown in Table 2, all chemical element contents coincide with the ASTM B275-02 standard specification (Ref. 14).

Tensile Test

In this study, the tensile test played the most important role, which used a direct measurement of UTS of the weldment in order to understand the influences of beam current, accelerating voltage, welding speed, and focal position. As shown in Figs. 2 and 3, the UTS of SC samples of AZ61A alloy clearly increases with increasing beam current and accelerating voltage, whereas it decreases with increasing welding speed. When the power is below 4000 W, this will cause incomplete joint penetration and result in occurrence of SC. But if the power is between 4000 and 5000 W, the strength of the samples remained constant over nearly the entire period studied. While the fixed accelerating voltage or beam current is individually changed to another condition (30, 40 kV or 125, 150 mA), they will have the similar trend. However, whether for changing the condition or not, the UTS of NSC samples have no obvious difference and its curves almost keep horizontal. For reasons stated above, there was no other special phase transformation in the weld when different energy was input by EBW.

Figure 4 shows the differences of weld appearance at different focal positions. Because the boiling point (1090°C) and melting point (650°C) of pure magnesium are lower than general engineering materials, while the energy density of EBW is higher than other arc welding, the AZ61A alloy in the weld will exhibit better fluidity during melting. At this time if the focal position of the electron beam is close to the top surface of the workpiece, the weld will produce worse spatter on the surface and lead to more apparent incomplete joint penetration at the root. Since these areas will incur severe stress concentration, UTS values of the samples from top to bottom approach 175.5 MPa (Fig. 4A), 242.8 MPa (Fig. 4B), and 247.5 MPa (Fig. 4C) in that order. This indicates an accurate reflection of actual conditions.

Judging from the above, the control parameters of the maximum value of UTS could be optimized with a beam current of 100 mA, accelerating voltage of 50 kV, welding speed of 60.6 mm/s, and focal position at bottom. The maximum value (247.5 MPa) of UTS for all SC samples

Table 1 — List of 77 sets of Parameters for EBW of AZ61A Extruded Plates

Code	Acceleration Voltage (kV)	Beam Current (mA)	Power (W)
A	50.0	100.0	
B	40.0	125.0	
C	33.3	150.0	5000
D	30.0	167.0	
E	50.0	90.0	
F	45.0	100.0	
G	40.0	113.0	4500
H	36.0	125.0	
I	30.0	150.0	
J	50.0	80.0	
K	40.0	100.0	
L	32.0	125.0	4000
M	30.0	133.0	
N	26.7	150.0	
O	50.0	70.0	
P	40.0	88.0	
Q	35.0	100.0	
R	30.0	117.0	3500
S	28.0	125.0	
T	23.3	150.0	
U	50.0	60.0	
V	40.0	75.0	
W	30.0	100.0	3000
X	24.0	125.0	
Y	20.0	150.0	

NOTE: A weldment with maximum UTS is selected from these coding parameters with 60.6, 73.3, and 86.0 mm/s with focus at bottom, and then it is compared with focusing at surface and middle of the plate.

Table 2 — Chemical Compositions of AZ61A Alloy as Measured by ICP-AES and ICP-MS (wt-%)

Element/ Material	Mg	Al	Zn	Mn	Si	Cu	Fe	P	Pb
AZ61A	93.0585	5.8800	0.7985	0.2205	0.0240	0.0007	0.0030	0.0012	0.0062

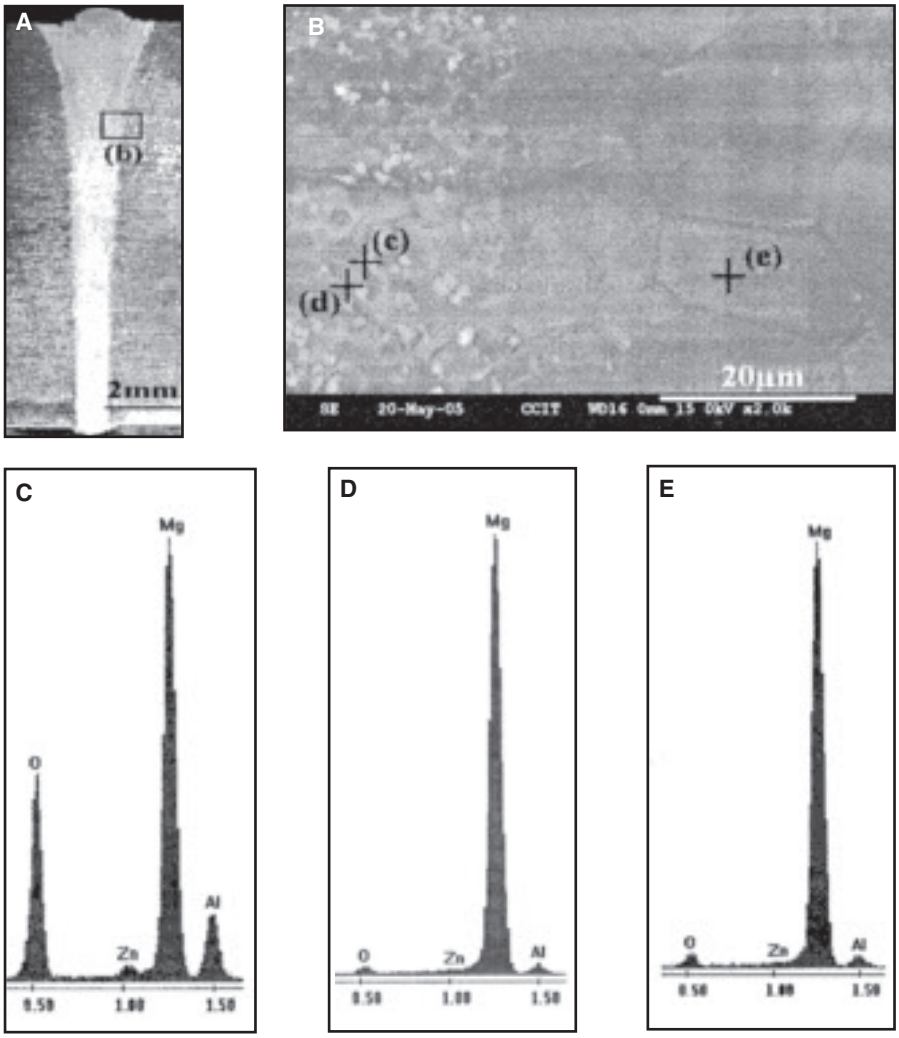

Fig. 5 — Microstructure observation and EDS analysis for the cross section of optimum weld. A — Cross section; B — SEM photograph at the weld boundary; EDS analysis. C — Particle; D — particle vicinity; E — base metal.

for base material, and the average value of UTS (286.0 MPa) for all NSC samples would reach 96% of UTS for the base metal. There was evidence showing that the impingement of SC reached at least 13% of UTS for the base metal. The follow-up experimental results discussed below further explain the remaining 4%. On the contrary, the UTS of the worst weldment reached only 168.1 MPa under the situation of complete joint penetration. Its parameters include a beam current of 100 mA, an accelerating voltage of 45 kV, a welding speed of 86.0 mm/s, and the focal position at the bottom.

Microstructure Observation

Figures 5 and 6 show the microstructures of the optimum and the worst weld cross section, respectively. The mean grain size of the FZ, HAZ, and base metal are 10, 20, and 15 μm, respectively. The small-sized equalaxial grain forms in the FZ (without columnar grain) due to the fast cooling of EBW. On the other hand, the HAZ has the largest grain and it precipitates some submicron-sized crystals in an annealing effect. Many precipitates are observed and concentrated in the FZ — Fig. 5B. Using energy-dispersive spectrometer (EDS) analysis, the chemical compositions of these precipitates (Fig. 5C) with more Al and Zn content than that of the base metal (Fig. 5E) were moved from the vicinity of these precipitates — Fig. 5D. Their Al content levels were 9.43, 4.80, and 5.81 wt-%, respectively; and their Zn content levels were 3.01, 1.57, and 2.37 wt-%, respectively.

The root concavity (Fig. 6A) and cavities (Fig. 6B) became the critical factors for weld fracture, which would cause excessive SC and reduce the UTS value of weldments. Visual inspections reveal that the fracture surfaces of all weldment tensile samples can be divided into two modes: the irregular FZ fracture (48%) and the regular HAZ fracture (52%). In the former mode, cracks running randomly across the middle of the weld are initiated and terminated in an undercut, HAZ, or root concavity. In the latter mode, a break occurs along the weld boundary.

In the Mg-Al binary phase diagram, the maximum solid solubility of aluminum is 11.5 wt-% at 437°C. It decreases to about 2 wt-% at room temperature. After solidification, 6% of Al element can be held in solid solution from 525° to 300°C in AZ61A alloy. $Mg_{17}Al_{12}$ does not precipitate near the grain boundary until the temperature is below 300°C. According to the authors' previous study (Ref. 15), the Vickers hardness of the weld is mainly affected by many brittle precipitates, which vary from scattered particles to dense dendrites as the Al content increases. With regard to the fracture modes of AZ61A alloy, it mainly depends on the distribution (denseness or scattering) of precipitates in FZ.

XRD Analysis

The preferred orientation and specific phase of these samples can be analyzed by XRD. As shown in Fig. 7, there is no formation of other phases in the unwelded or welded samples, and there is very little differences between the optimum and the worst weldments. It is found that the high fraction of (1 0 $\bar{1}$ 1) and (1 0 $\bar{1}$ 0) planes lie on the transverse plane of AZ61A extruded plate before EBW. However, after using EBW, the preferred orientation in FZ will remain only in the (1 0 $\bar{1}$ 1) plane, and the (0 0 0 2) orientation will increase with stepwise diffraction intensity. It follows that the γ phase ($Mg_{17}Al_{12}$) is the sole intermetallic compound whose peak is beside (1 0 $\bar{1}$ 1), and the weldments will not form any other phase transformation that affects its UTS. According to the experimental results of 77 sets of specimens, there were two different kinds of fracture modes in the tensile tests. Some parts broke along the HAZ, while others cracked randomly across the middle of the

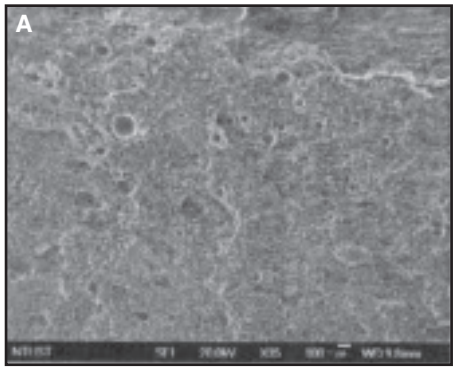

Fig. 6 — Microstructure observation of the worst weld. A — Cross section; B — SEM photograph at the fracture face of the weld.

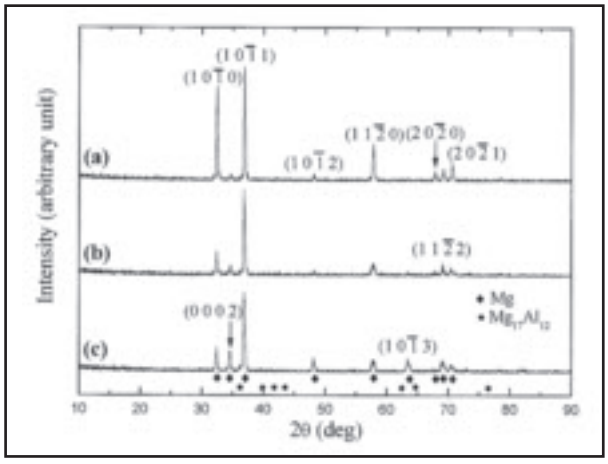

Fig. 7 — Comparison of XRD spectrum for prewelding and postwelding samples of AZ61A-F. A — Prewelding sample; B — optimum weld sample; C — worst weld sample.

weld with initial and terminal positions located in the HAZ or root concavity. This phenomenon clarified that the distribution of γ phase and cavities in the weld would influence the strength of the weldment.

Micro-Indentation Hardness Test

The positions for micro-indentation hardness tests are indicated in Fig. 8A, with the results presented in Fig. 8B. It can be seen that the hardness is high in the center of the upper weld, and decreases toward the bottom of the sample and away from the FZ axis because of the spatial distribution of the brittle γ phases. Moreover, the curve of the optimum sample is more symmetrical than the worst one. This may be because of the softening effect of annealing in the HAZ and the existence of cavities in the weld together caused the larger area of indentation and thus influenced the test value of the micro-indentation hardness. Therefore, there was a sudden dip in the random positions of the HAZ. From this viewpoint, the crack initiation and propagation in AZ61A weldments would also occur in the HAZ. In other words, the HAZ would be the main reason that the UTS reduced at least 4% in the base metal for NSC weldment.

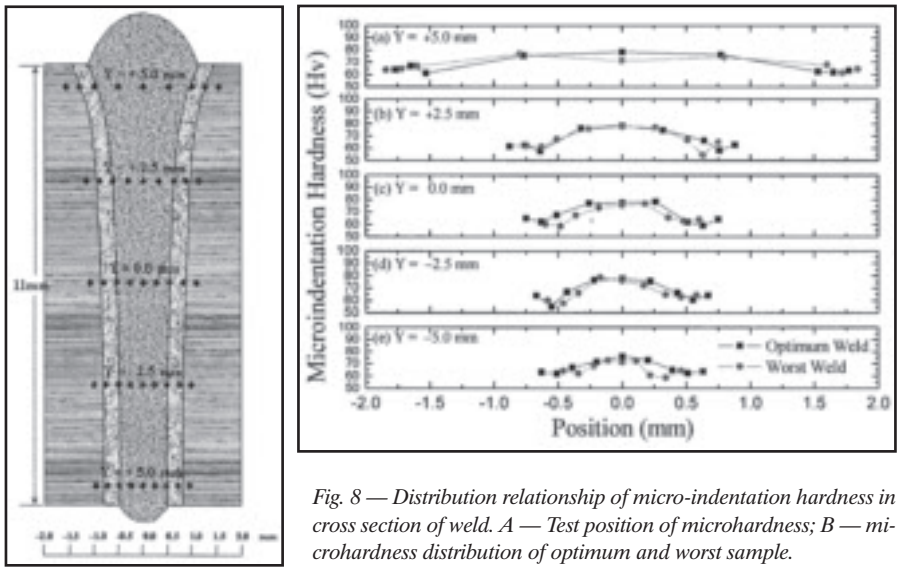

Fig. 8 — Distribution relationship of micro-indentation hardness in cross section of weld. A — Test position of microhardness; B — microhardness distribution of optimum and worst sample.

Conclusions

In this study, the parameters were optimized with a beam current of 100 mA, accelerating voltage of 50 kV, welding speed of 60.6 mm/s, and focal position at the bottom. The maximum value (247.5 MPa) of the UTS for the SC weldment of AZ61A-F and the average value (286.0 MPa) of the UTS for the NSC weldment of AZ61A-F resulted in 83% and 96% of UTS for the base metal, respectively. The harmful influence of SC and HAZ reached at least 13% and 4%, respectively, of the UTS for the base metal.

The power was suitable between 4000 and 5000 W for welding 11-mm-thick AZ61A extruded plates. Under worst conditions, the UTS of EBW on AZ61A extruded plates was reduced by the three factors of root concavity, HAZ, and cavities.

Acknowledgments

The authors heartily acknowledge the support from the National Science Council, ROC., under Project No. NSC 93-2623-7-182-002. The authors also thank C. L. Chang and Z. G. Chang of System Manufacturing Center of Chung-Shan Institute of Science and Technology for technical assistance.

References

1. Avedesian, M. M., and Baker, H. 1999. *Magnesium and Magnesium Alloys.* ASM International, Materials Park, Ohio.

2. Sun, Z., Wei, J., Pan, D. Y., and Tan, Y. K. 2002. Comparative evalution of tungsten inert gas and laser welding of AZ31B magnesium alloy. *Science and Technology of Welding and Joining* 7(6): 343–351.

3. Weisheit, A., Galun, R., and Mordike, B. L. 1998. CO_2 laser beam welding of magnesium-based alloys. *Welding Journal* 77(4): 149–154.

4. Pan, L. K., Wang, C. C., Hsiao, Y. C., and Ho, K. C. 2004. Optimization of Nd: YAG laser welding onto magnesium alloy via taguchi analysis. *Optics & Laser Technology* 37: 33–42.

5. Pan, L. K., Wang, C. C., Shin, Y. C., and Sher, H. F. 2005. Optimizing multiple qualities of Nd: YAG laser welding onto magnesium alloy via grey relational analysis. *Science and Technology of Welding and Joining* 10(4): 1–8.

6. Sun, Z., and Karppi, R. 1996. The application of electron beam welding for the joining of dissimilar metals: An overview. *Journal of Materials Processing Technology* 59: 257–267.

7. Haferkamp, H., Dilthey, U., Träger, G., Burmester, I., and Niemeyer, M. 1998. Beam welding of magnesium alloys. *Magnesium Al-*

loys and Their Application. Eds. B. L. Mordike and K. U. Kainer, pp. 595–600, Werkstoff-Informationsgesellschaft.

8. Dilthey, U., and Weiser, J. 1997. Investigations of EB characteristics and their influences on the weld shape. *Welding in the World* 39(2): 89–98.

9. Su, S. F., Huang, J. C., Lin, H. K., and Ho, N. J. 2002. Electron beam welding behavior in Mg-Al based alloys. *Metallurgical and Materials Transactions* 33A: 1461–1473.

10. Guenther, S., and Armando, J. 2001. Electron beam welding of die cast magnesium. *Advanced Materials & Processes* 159(8): 67–69.

11.Vogelei, C., Dobeneck, D., Decker, I., and Wohlfahrt, H. 2000. Strategies to reduce porosity in electron beam welds of magnesium die-casting alloys. *Magnesium Alloys and their Application*. Ed. K. U. Kainer, pp. 191–199, WILEY-VCH.

12. Draugelates, U., Bouaifi, B., Bartzsch, J., and Ouaissa, B. 1998. Properties of nonvacuum electron beam welds of magnesium alloys. *Magnesium Alloys and their Application*. Eds. B. L. Mordike and K. U. Kainer, pp. 601– 606. Werkstoff-Informationsgesellschaft.

13. American Society for Testing and Materials. 2002. *Standard Test Method of Tension Testing Wrought and Cast Aluminum and Magnesium Alloy Products*. ASTM B557-02.

14. American Society for Testing and Materials. 2002. *Standard Practice for Codification of Certain Nonferrous Metals and Alloys Cast and Wrought*. ASTM B275-02.

15. Chi, C. T., Chao, C. G., Liu, T. F., and Wang, C. C. 2006. A study of weldability and fracture modes in electron beam weldments of AZ series magnesium alloys. *Materials Science and Engineering* 435-436A. 672–680.

The 2007 World Standards Day Paper Competition

The Standards Engineering Society (SES) has established the theme of this year's World Standards Day Paper Competition as "Standards and the Global Village." For many decades, standards have successfully created international consensus on critical issues such as consumer information and protection, the quality and safety of products and services, the environment, health care, security, Internet protocols, and fair trade, among others. The 2007 competition invites papers that show, using specific examples, ways that standards developing organizations have encouraged and created global consensus for the economic and social benefit of the global village.

Paper competition winners will be announced and given their awards at the U.S. celebration of World Standards Day, which will be held this year on October 18, at the Ronald Reagan Building and International Trade Center in Washington, D.C.

Cash prizes are awarded by SES and the World Standards Day Planning Committee for the best three papers submitted. The first place winner will receive a plaque and $2500. second and third place winners will receive $1000 and $500, respectively, along with a certificate. In addition, the winning papers will be published in SES's journal, *Standards Engineering*.

All paper contest submissions must be received with an official entry form by midnight August 31, 2007, by the SES Executive Director, 13340 SW 96th Avenue, Miami, Fla., 33176. For details on the winners' recognition, cash awards, judging, and rules, go to *www.ses-standards.org* and follow the link for 2007 WSD Paper Competition.

CAN WE TALK?

The *Welding Journal* staff encourages an exchange of ideas with you, our readers. If you'd like to ask a question, share an idea or voice an opinion, you can call, write, e-mail or fax. Staff e-mail addresses are listed below, along with a guide to help you interact with the right person.

Publisher/Editor
Andrew Cullison
cullison@aws.org, Extension 249
Article Submissions

Senior Editor
Mary Ruth Johnsen
mjohnsen@aws.org, Extension 238
Feature Articles

Associate Editor
Howard Woodward
woodward@aws.org, Extension 244
Society News
Personnel

Assistant Editor
Kristin Campbell
kcampbell@aws.org, Extension 257
New Products
News of the Industry

Managing Editor
Zaida Chavez
zaida@aws.org, Extension 265
Design and Production

Advertising Sales Director
Rob Saltzstein
salty@aws.org, Extension 243
Advertising Sales

Advertising Sales & Promotion Coordinator
Lea Garrigan Badwy
garrigan@aws.org, Extension 220
Production and Promotion

Advertising Production Manager
Frank Wilson
fwilson@aws.org, Extension 465
Advertising Production

Peer Review Coordinator
Erin Adams
eadams@aws.org, Extension 275
Peer Review of Research Papers

Welding Journal Dept.
550 N.W. LeJeune Rd.
Miami, FL 33126
(800) 443-9353
FAX (305) 443-7404